Enhancement of pump efficiency of a visible wavelength organic distributed feedback laser by resonant optical pumping

Chun Ge,[1] Meng Lu,[2] Yafang Tan,[1] and Brian T. Cunningham[1,3,*]

[1]*Department of Electrical and Computer Engineering, University of Illinois at Urbana-Champaign, Urbana, Illinois, USA*

[2]*SRU Biosystems, Woburn, Massachusetts, USA*

[3]*Department of Bioengineering, University of Illinois at Urbana-Champaign, Urbana, Illinois, USA*

**bcunning@illinois.edu*

Abstract: A 22× reduction in laser pump threshold and a 23× enhancement in energy conversion have been demonstrated on a second order distributed feedback (DFB) laser using a resonant optical pumping (ROP) technique. The ROP scheme couples the excitation light into a distinct resonant mode of the laser cavity through the illuminating at a specific resonant incident angle. Coupling excitation light into the resonant mode results in an enhanced near-field, which significantly increases pump absorption by the active medium. Consequently, high power conversion efficiency between pumping light and lasing emission is achieved and laser pump threshold power is reduced.

OCIS codes: (140.3490) Lasers, distributed-feedback; (050.0050) Diffraction and gratings; (260.2160) Energy transfer.

References and links

1. T. H. Maiman, "Stimulated optical radiation in ruby," Nature **187**(4736), 493–494 (1960).
2. F. Martini, G. Innocenti, G. Jacobovitz, and P. Mataloni, "Anomalous spontaneous emission time in a microscopic optical cavity," Phys. Rev. Lett. **59**(26), 2955–2958 (1987).
3. C. Karnutsch, C. Gyrtner, V. Haug, U. Lemmer, T. Farrell, B. S. Nehls, U. Scherf, J. Wang, T. Weimann, G. Heliotis, C. Pflumm, J. C. deMello, and D. D. C. Bradley, "Low threshold blue conjugated polymer lasers with first- and second-order distributed feedback," Appl. Phys. Lett. **89**(20), 201108 (2006).
4. N. Tsutsumi and M. Yamamoto, "Threshold reduction of a tunable organic laser using effective energy transfer," J. Opt. Soc. Am. B **23**(5), 842–845 (2006).
5. B. K. Yap, R. Xia, M. Campoy-Quiles, P. N. Stavrinou, and D. D. C. Bradley, "Simultaneous optimization of charge-carrier mobility and optical gain in semiconducting polymer films," Nat. Mater. **7**(5), 376–380 (2008).
6. E. B. Namdas, M. Tong, P. Ledochowitsch, S. R. Mednick, J. D. Yuen, D. Moses, and A. J. Heeger, "Low thresholds in polymer lasers on conductive substrates by distributed feedback nanoimprinting: Progress toward electrically pumped plastic lasers," Adv. Mater. **21**(7), 799–802 (2009).
7. R. Harbers, P. Strasser, D. Caimi, R. F. Mahrt, N. Moll, B. J. Offrein, D. Erni, W. Bachtold, and U. Scherf, "Enhanced feedback in organic photonic-crystal lasers," Appl. Phys. Lett. **87**(15), 151121 (2005).
8. M. H. Song, D. Kabra, B. Wenger, R. H. Friend, and H. J. Snaith, "Optically-pumped lasing in hybrid organic-inorganic light-emitting diodes," Adv. Funct. Mater. **19**(13), 2130–2136 (2009).
9. M. J. Bohn and J. G. McInerney, "Resonant optical pumping of vertical-cavity surface-emitting lasers," Opt. Commun. **117**(1-2), 111–115 (1995).
10. F. De Martini and G. Jacobovitz, "Anomalous spontaneous-stimulated-decay phase transition and zero-threshold laser action in a microscopic cavity," Phys. Rev. Lett. **60**(17), 1711–1714 (1988).
11. G. Heliotis, R. Xia, G. A. Turnbull, P. Andrew, W. L. Barnes, I. D. W. Samuel, and D. D. C. Bradley, "Emission characteristics and performance comparison of polyfluorene lasers with one- and two-dimensional distributed feedback," Adv. Funct. Mater. **14**(1), 91–97 (2004).
12. V. Sandoghdar V, F. Treussart, J. Hare, V. Lefèvre-Seguin V, J. M. Raimond, and S. Haroche, "Very low threshold whispering-gallery-mode microsphere laser," Phys. Rev. A **54**(3), R1777–R1780 (1996).
13. M. Kuwata-Gonokami, R. H. Jordan, A. Dodabalapur, H. E. Katz, M. L. Schilling, R. E. Slusher, and S. Ozawa, "Polymer microdisk and microring lasers," Opt. Lett. **20**(20), 2093–2095 (1995).
14. F. Raineri, G. Vecchi, A. M. Yacomotti, C. Seassal, P. Viktorovitch, R. Raj, and A. Levenson, "Doubly resonant photonic crystal for efficient laser operation: Pumping and lasing at low group velocity photonic modes," Appl. Phys. Lett. **86**(1), 011116 (2005).

#140703 - $15.00 USD Received 7 Jan 2011; revised 13 Feb 2011; accepted 21 Feb 2011; published 2 Mar 2011

15. C. H. Henry, R. F. Kazarinov, R. A. Logan, and R. Yen, "Observation of destructive interference in the radiation loss of second-order distributed feedback lasers," IEEE J. Quantum Electron. **21**(2), 151–154 (1985).
16. M. Lu, S. Choi, C. J. Wagner, J. G. Eden, and B. T. Cunningham, "Label free biosensor incorporating a replica-molded, vertically emitting distributed feedback laser," Appl. Phys. Lett. **92**(26), 261502 (2008).
17. C. Ge, M. Lu, W. Zhang, and B. T. Cunningham, "Distributed feedback laser biosensor incorporating a titanium dioxide nanorod surface," Appl. Phys. Lett. **96**(16), 163702 (2010).
18. C. Ge, M. Lu, X. Jian, Y. Tan, and B. T. Cunningham, "Large-area organic distributed feedback laser fabricated by nanoreplica molding and horizontal dipping," Opt. Express **18**(12), 12980–12991 (2010).
19. B. Park and M. Y. Han, "Organic light-emitting devices fabricated using a premetered coating process," Opt. Express **17**(24), 21362–21369 (2009).
20. J. Faist, C. Gmachl, F. Capasso, C. Sirtori, D. L. Sivco, J. N. Baillargeon, and A. Y. Cho, "Distributed feedback quantum cascade lasers," Appl. Phys. Lett. **70**(20), 2670–2672 (1997).
21. H. Kogelnik and C. V. Shank, "Coupled-wave theory of distributed feedback lasers," J. Appl. Phys. **43**(5), 2327–2335 (1972).
22. E. Kapon, A. Hardy, and A. Katzir, "The effect of complex coupling coefficients on distributed feedback lasers," IEEE J. Quantum Electron. **18**(1), 66–71 (1982).

1. Introduction

Increased pump efficiency has been an important research topic since the first demonstration of lasing in1957 [1–9]. Enhancement of pump efficiency benefits both energy conversion and lasing pump threshold, which is defined as the lowest input energy at which the sum of all the losses experienced by the light in one round trip is balanced by the optical gain of the lasing medium. Many previous approaches for pump threshold reduction have concentrated upon designing small mode-volume and high *Q*-factor optical cavities with strong optical confinement [10,11], such as vertical cavities with distributed Bragg reflectors [11], two dimensional (2D) photonic crystal (PC) microcavities [7], and whispering-gallery mode oscillators [12,13]. A drawback of using high *Q* cavities, however, is that the low out-coupling efficiency also reduces the slope efficiency of the laser. Recently, more efficient pump methods were developed to optically excite 2D PC [14] and vertical cavity lasers [9] by matching the wavelength of illumination with the resonant wavelength of the cavity.

Here, we present a resonant optical pumping (ROP) scheme for the distributed feedback laser which simultaneously reduces the laser pump threshold while enhancing the energy conversion efficiency by increasing the pumping absorption efficiency. The ROP technique couples the excitation light into a distinct resonant mode of the laser cavity through illumination at a specific resonant incident angle. Coupling excitation light into the resonant mode results in an enhanced near-field, which significantly increases pump absorption by the active medium. Consequently, high power conversion efficiency between pumping light and lasing emission is achieved and laser pump threshold power is reduced. For a given pump power, the ROP approach decreases the laser pumping threshold and improves the slope efficiency through enhanced pumping absorption efficiency, without changing the output coupling efficiency. While tuning of the excitation wavelength has been used successfully to improve pump efficiency for 2D photonic crystal slab lasers [14] and vertical cavity lasers, the incident angle tuning approach described in this work is simple to implement with a non-tunable pump laser, as one need only to choose the correct angle of incidence.

2. Device structure and fabrication

Due to its ability to provide efficient distributed reflection with an easily fabricated corrugated periodic refractive index structure, the DFB structure has become a popular narrow linewidth light source for optical communications. Embossing, imprinting, and nanoreplica molding techniques have simplified the fabrication process for defining the sub-wavelength dimensions required for the DFB structure, and plastic-based devices have been demonstrated through incorporation of dye doping within an active polymer medium. The particular DFB structure studied in this paper incorporates a second order Bragg grating. Unlike first order DFB structures, second order gratings couple cavity modes into surface-emitting modes by first order diffraction [15]. Due to the phase matching condition, each wavelength couples resonantly with the structure for a distinct angle of incidence. While the surface-emitting

#140703 - $15.00 USD Received 7 Jan 2011; revised 13 Feb 2011; accepted 21 Feb 2011; published 2 Mar 2011

mode is used to extract light out of the cavity, the same DFB structure also supports an off-normal resonant mode which can couple resonantly with an external optical pump source.

A cross-sectional diagram (not to scale) of the DFB laser is shown in Fig. 1. A one-dimensional (1D) surface grating structure is formed in an ultraviolet curable polymer (UVCP) upon a flexible polyethylene-terephthalate (PET) substrate by nanoreplica molding [16,17]. The polymer grating surface is coated by horizontal dipping [18,19] with a high refractive index polymer layer, SU-8 (Microchem) doped with Rhodamine-590, (~1% wt%, Exciton) which functions as the gain medium. The gain layer has an overall thickness of ~400 nm and a refractive index of n = 1.58. Finally, a 20 nm titanium dioxide (TiO_2) thin film is deposited on top of the DFB laser surface by electron beam evaporation. The TiO_2 film is used in the context of operating this device as a label-free biosensor [17], in order to vertically displace the resonant mode into media (water) on top of the DFB surface as a means for increasing detection sensitivity.

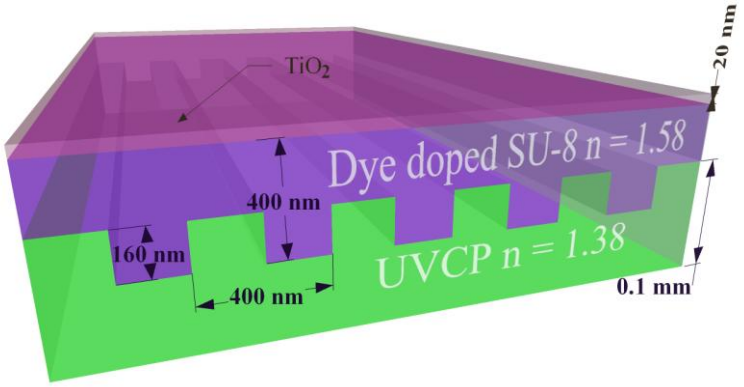

Fig. 1. Schematic diagram of the surface-emitting DFB laser.

3. Band structure and near field calculation

Under broadband illumination, a highly efficient reflection represents a resonance supported by the DFB cavity at a specific wavelength and a specific angle. A simulation tool (DiffractMOD, RSoft Design Group) based on the rigorous coupled-wave analysis (RCWA) technique aids the identification of the resonant modes. Figure 2 (a) shows a photonic band diagram for the structure described in Fig. 1, calculated for transverse electric (TE) modes in the $500 < \lambda < 680$ nm wavelength interval and the radiation angle, θ, varied from 0° to 12°. Generally, the complex-coupled organic DFB laser facilitates single mode yield by removing the mode degeneracy that exists in pure index coupled or pure gain coupled DFB lasers [20–22]. From the photonic band diagram, an emission wavelength of $\lambda = 584$ nm and a resonant incident angle of 9.13° for the excitation laser at $\lambda = 532$ nm can be predicted. Figure 3(a) and (b) show the simulated near electric field intensity (normalized to the intensity of incident field) for the excitation light coupled into resonance from 9.13° and excitation light coupled at an off-resonant angle of 0°. The influence of the resonance phenomenon on the resulting near-fields is clearly manifested in the electric field intensity, where resonant pumping results in ~81 × greater electric field intensity within the gain medium than ordinary non-resonant pumping. The photonic band diagram of the fabricated device was measured by illuminating with collimated white light and measuring the transmitted spectrum with a spectrometer (HR 4000, Ocean Optics) as a function of the incident angle. The consequent band diagram is shown in Fig. 2 (b), which agrees well with the simulated band diagram shown in Fig. 2 (a).

#140703 - $15.00 USD Received 7 Jan 2011; revised 13 Feb 2011; accepted 21 Feb 2011; published 2 Mar 2011

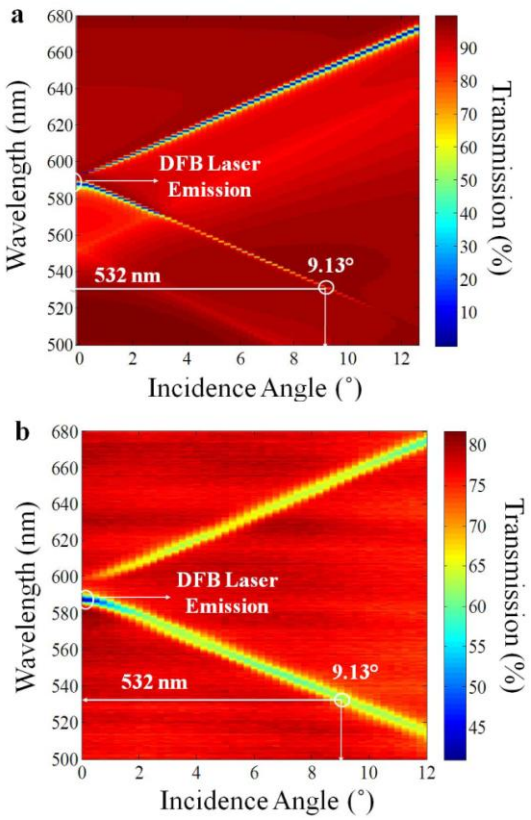

Fig. 2. Photonic band diagram of the DFB laser. (a), resonant mode dispersion calculated using RCWA. Simulation results identify the resonant pumping angle at 9.13° for the excitation mode λ = 532 nm and the vertically emitting mode λ = 584 nm. All angles are measured with respect to the normal of the surface grating in Fig. 1. (b), measured photonic dispersion of the resonant modes. The experimentally obtained data suggests that the pumping light at λ = 532 nm couples to the resonant mode by following the photonic dispersion.

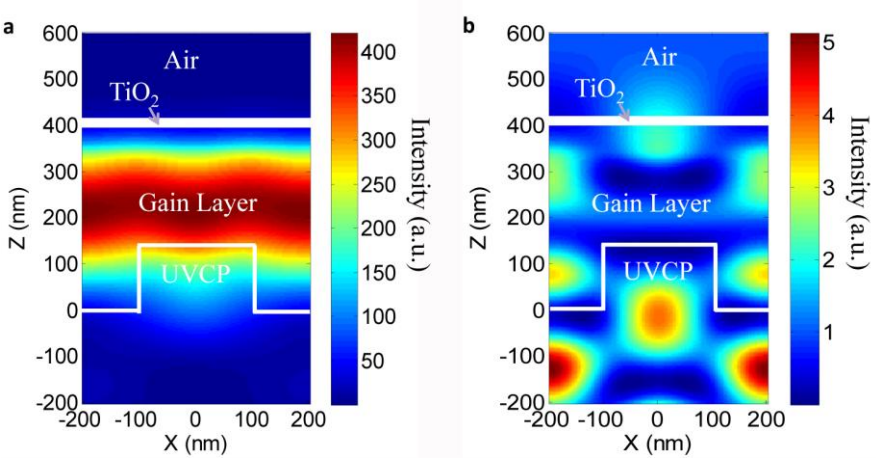

Fig. 3. Near-field intensity calculation. Electric field intensity profile calculated using RCWA for the TE pumping mode at λ = 532 nm under resonant pumping condition (a), and non-resonant pumping condition (b). Note different colorbar scales are used.

#140703 - $15.00 USD Received 7 Jan 2011; revised 13 Feb 2011; accepted 21 Feb 2011; published 2 Mar 2011

4. Experimental results

The DFB laser was pumped with a frequency-doubled, *Q*-switched Nd: YAG pulse laser (λ = 532 nm, yttrium aluminum garnet) with pulse duration of 10 ns at a repetition rate of 2 Hz. The excitation spot size and pump fluence were controlled by an adjustable pinhole and a continuous variable neutral density filter (OD 0-4.0). The DFB laser emission was normal to the device surface and was coupled by a convex lens into a step index multimode fiber with a high numerical aperture (NA = 0.48). The laser output was then analyzed by a spectrometer (HR4000, Ocean Optics) with a resolution of 0.12 nm.

In order to demonstrate the effect of ROP on the fabricated DFB laser, the dependence of the relative DFB laser pulse energy upon the pump fluence was investigated. Figure 4 shows the narrow-band emission of the laser when pumped above threshold. As illustrated by Fig. 5, above threshold, the output energy rises linearly with pump energy illuminated from four different incident angles. Using a linear least-squares fit to the emission fluence above threshold, clear threshold energies of 0.34 μJ/mm^2, 0.55 μJ/mm^2, 3.59 μJ/mm^2, and 7.48 μJ/mm^2 were found for excitations from 9.13°, 9.08°, 9.03° and 0°. The inset of Fig. 5 summarizes the laser pumping threshold and the laser slope efficiency as a function of the excitation angle of the pump light. Both laser pumping threshold and slope efficiency change dramatically with the pumping angle. On the basis of the inset of Fig. 5, the laser pump threshold drops 22 × when pumped at the resonance angle (9.13°) compared to the case without using resonance (0°). Meanwhile, the slope efficiency is enhanced by 23 × at resonance. In order to ensure that the same location was reproducibly excited under different pumping angles, the device was placed on a rotation stage (PR01, Thorlabs) with the device surface overlapping the rotation axis and the pumping light was designed to pass through the rotation axis at a right angle.

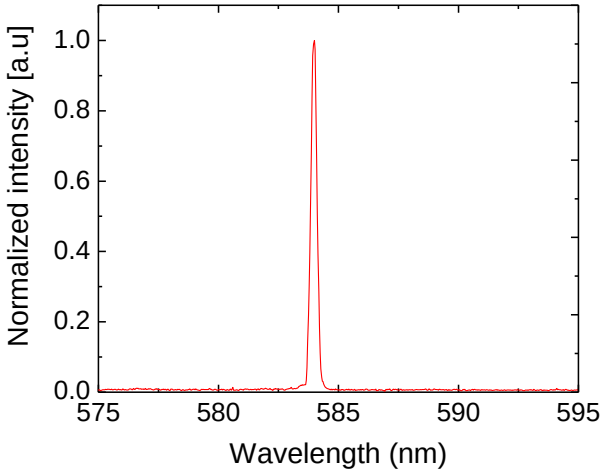

Fig. 4. A typical above-threshold emission spectrum from the device.

#140703 - $15.00 USD Received 7 Jan 2011; revised 13 Feb 2011; accepted 21 Feb 2011; published 2 Mar 2011

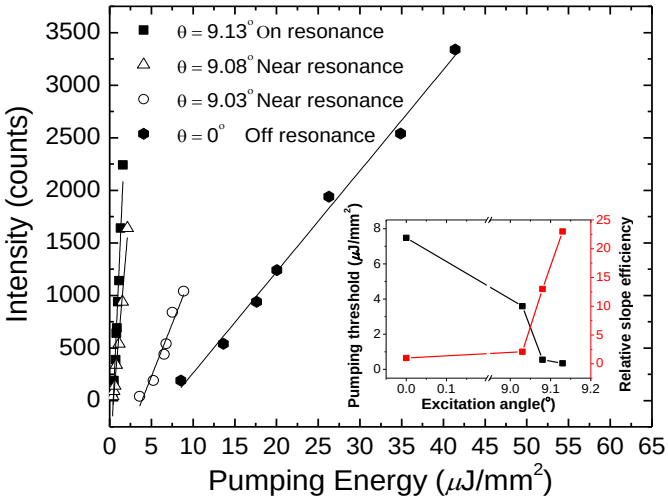

Fig. 5. Emission characteristics of a surface-emitting DFB laser in terms of the pumping angle. The inset plot depicts the laser pumping threshold and the slope efficiency as a function of the pumping angle. Threshold energies of ~0.34 μJ/mm^2, 0.55 μJ/mm^2, 3.59 μJ/mm^2, and 7.48 μJ/mm^2 were found for excitations from 9.13° (on resonance), 9.08° (near resonance), 9.03° (near resonance) and 0° (off resonance), using a linear least-squares fit to the experimentally obtained data. Fitting results indicate a 22 × reduction in the pump threshold energy for lasing when pumped at the resonance angle (9.13°) compared to the case without using resonance (at 0°). Meanwhile, the slope efficiency is enhanced by 23 × at resonance, according to the linear fitting.

The relationship between the absorption efficiency and the pumping angle has also been investigated with measurement results shown in Fig. 6. In order to accurately measure the absorption efficiency, a continuous wave (CW) Nd: YAG laser with output power of 5 mW was utilized as the excitation source during this experiment. The power of the incident, reflected, and transmitted light was measured using a Si photodiode based power and energy meter (PM320E, Thorlabs). Under resonant pumping, the absorption efficiency was maximized and was ~31.65%. While at normal incidence, the absorption efficiency was only ~1.37% (not shown in Fig. 6). Therefore, the absorption efficiency could be increased by ~23 × simply by implementing resonant pumping without changing the device configuration. Additionally, the curve characterizing the relationship between the absorption and the pumping angle agrees well with the relationship observed between the laser emission intensity and the pump incident angle. This agreement indicates that the reduced laser pumping threshold and improved slope efficiency result from the increased pump energy absorption. This increased energy absorption will enhance the resonant electromagnetic field inside the gain layer, which in turn will dramatically decrease the laser pump threshold power and improve the slope efficiency.

#140703 - $15.00 USD Received 7 Jan 2011; revised 13 Feb 2011; accepted 21 Feb 2011; published 2 Mar 2011

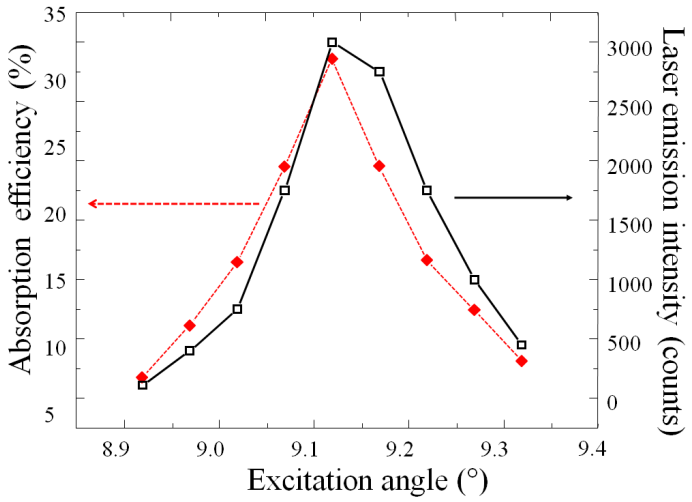

Fig. 6. Absorption efficiency and laser output versus the pumping angle. Both the absorption efficiency of the pumping energy and the laser output peak at the resonant excitation angle (9.13°) and drop in the same manner as the pumping light shifts away from the resonant incident angle. This agreement indicates that it is the increased pumping energy absorption that results in the reduced lasing threshold and the improved slope efficiency.

Resonant pumping is not limited to 1D DFB lasers, as the concept may be extended to other cavity structures, such as microrings, microspheres microtoroids lasers, 2D DFB surfaces, and 2D photonic crystal lasers. In principle, the ROP technique can be applied to any laser cavity with co-existing modes at the wavelength of laser emission and the pump wavelength to reduce the pumping threshold and to increase the slope efficiency. However, it should be noted that the effects of reduced threshold and increased slope efficiency are strongly dependent upon the spatial overlap between the resonant pumping mode and the lasing mode. If the spatial overlap between these two modes is poor, the effects of ROP will be minimized.

5. Acknowledgement

This work was supported the U.S. Army Medical Research and Materiel Command (USAMRMC), the Telemedicine and Advanced Technology Research Center (TATRC) under Contract W81XWH0810701 and the National Science Foundation under Grant No. 0427657. C. Ge and M. Lu contributed equally to this work.